Correspondence between sound propagation in discrete and continuous random media with application to forest acoustics

Journal Item

Correspondence between sound propagation in discrete and continuous random media with application to forest acoustics

Vladimir E. Ostashev, D. Keith Wilson, Michael B. Muhlestein, and Keith Attenborough

Citation: The Journal of the Acoustical Society of America **143**, 1194 (2018); doi: 10.1121/1.5024904
View online: https://doi.org/10.1121/1.5024904
View Table of Contents: http://asa.scitation.org/toc/jas/143/2
Published by the Acoustical Society of America

Correspondence between sound propagation in discrete and continuous random media with application to forest acoustics

Vladimir E. Ostashev,[a] D. Keith Wilson, and Michael B. Muhlestein
United States Army Engineer Research and Development Center, 72 Lyme Road, Hanover, New Hampshire 03755, USA

Keith Attenborough
Open University, Milton Keynes, MK7 6AA, United Kingdom

(Received 13 December 2017; revised 2 February 2018; accepted 2 February 2018; published online 26 February 2018)

Although sound propagation in a forest is important in several applications, there are currently no rigorous yet computationally tractable prediction methods. Due to the complexity of sound scattering in a forest, it is natural to formulate the problem stochastically. In this paper, it is demonstrated that the equations for the statistical moments of the sound field propagating in a forest have the same form as those for sound propagation in a turbulent atmosphere if the scattering properties of the two media are expressed in terms of the differential scattering and total cross sections. Using the existing theories for sound propagation in a turbulent atmosphere, this analogy enables the derivation of several results for predicting forest acoustics. In particular, the second-moment parabolic equation is formulated for the spatial correlation function of the sound field propagating above an impedance ground in a forest with micrometeorology. Effective numerical techniques for solving this equation have been developed in atmospheric acoustics. In another example, formulas are obtained that describe the effect of a forest on the interference between the direct and ground-reflected waves. The formulated correspondence between wave propagation in discrete and continuous random media can also be used in other fields of physics. https://doi.org/10.1121/1.5024904

[JFL] Pages: 1194–1205

I. INTRODUCTION

Sound propagation in a forest is a complicated phenomenon due to multiple scattering by trunks and branches, visco-thermal attenuation and induced vibration in the canopy, the ground effect, and micrometeorology. This problem is important in several applications such as noise reduction near highways by a stand of trees and localization of sound sources in forests. Recent overviews of forest acoustics can be found in Refs. 1 and 2.

Predicting sound propagation in a forest presents challenges. Most modeling is based on engineering approaches where different propagation factors are accounted for separately and their interactions are ignored. Finite-difference time-domain (FDTD) techniques have recently been applied to forest acoustics.[3–5] However, accurate numerical modeling of sound scattering by numerous scatterers in a forest is still computationally prohibitive. Therefore, it is desirable to develop rigorous methods for predicting forest acoustics, which are computationally feasible.

Due to the complexity of sound propagation in a forest, it is convenient to employ a stochastic approach by assuming that different scatterers, such as trunks and branches, have random locations. This enables the derivation of closed-form equations for the first two statistical moments of the sound field: the mean sound field and the spatial correlation function of the sound field (including the mean intensity). The second statistical moment is usually measured experimentally; the mean sound field can be used to approximate the mean intensity at relatively short propagation ranges. Note that a stochastic approach might not be applicable for forests in which the trees are planted in regular patterns.[4,6]

In the literature, two-dimensional (2D) multiple scattering theory has been used to calculate the mean sound field (e.g., Refs. 1,7–9). In this approach, the effective sound wavenumber k_{eff} due to sound scattering by trunks is obtained first. Then, sound propagation in a forest is represented as propagation in free space with the sound wavenumber replaced with k_{eff}.

Recently, three-dimensional (3D) multiple scattering theory has been employed in describing forest acoustics. In Ref. 10, the effective sound wavenumbers k_{eff} due to sound scattering by trunks, large branches, and the canopy were calculated. Trunks and large branches were approximated as vertical and slanted finite cylinders, while the canopy layer was modeled by diffuse scatterers. The mean sound field was then calculated for several cases of the problem with increasing complexity: sound propagation above an impedance ground in free space, a trunk layer added to the previous case, a canopy layer added above the trunk layer, and inclusion of the effective sound speed in the trunk and canopy layers. In Ref. 2, sound propagation in a forest was analyzed using the radiative transfer equation (RTE) for the second statistical moment of a sound field. The RTE can be derived from first principles using 3D multiple scattering theory. The RTE was solved in a modified Born approximation to calculate and analyze the mean sound intensity transmitted and reflected from a stand of

[a]Electronic mail: vladimir.ostashev@colorado.edu

trees.[2] A modified Born approximation was also used to study pulse propagation in a forest.[11]

The current paper continues the application of 3D multiple scattering theory to forest acoustics and has three main goals: (i) show the correspondence between equations describing the first two statistical moments of the sound field in a forest and a turbulent (random) atmosphere; (ii) using this correspondence, obtain new results for sound propagation in these media; and (iii) study the effect of sound scattering on the interference of the direct and ground-reflected waves in a forest.

Sound propagation in discrete and continuous random media, such as a forest and a turbulent atmosphere, is described by different starting equations. However, it has been noted in the literature (e.g., Refs. 12,13) that some equations for the statistical moments of the electromagnetic or sound field in discrete and continuous random media have a similar form. In the present paper, we build on these results and argue that the equations for the statistical moments of the sound field in a forest and turbulent atmosphere *should* have the same form if, in these equations, the scattering properties of the two media are expressed in terms of the differential scattering cross section (DSCS) and total cross section (TCS). This conclusion is also valid for wave propagation in many other discrete and continuous random media, and can be utilized in various applications such as sound scattering by air bubbles in water and urban acoustics.

The theories of sound propagation in a turbulent atmosphere have been well developed in the literature and summarized in Ref. 14. In the present paper, we use these theories and the abovementioned similarity between sound propagation in discrete and continuous random media to advance forest acoustics. Furthermore, some results from forest acoustics enable new formulations for sound propagation in a turbulent atmosphere.

As an important example, this paper considers the interference between the direct and ground-reflected waves in a forest. For typical, relatively soft forest floors this interference could theoretically result in significant reduction of sound levels.[7,15,16] However, in practice this reduction is not fully observed since scattering by trees results in a coherence loss between the direct and ground-reflected waves, thus, producing an apparent increase in sound levels. In Ref. 17, a heuristic approach was used to account for the loss of coherence between the direct and ground-reflected waves in a forest. A similar effect has been well studied for sound propagation in a turbulent atmosphere.[14,18–21] In the present paper, we use the latter theory to analyze a similar effect in a forest. This was also done in Ref. 22, in which the variance and the correlation length of the Gaussian-spectrum model of atmospheric turbulence were used as adjustable parameters for best fit between theoretical predictions and experimental data.

The paper is organized as follows. In Sec. II, the correspondence between equations for the statistical moments of the sound field in a forest and turbulent atmosphere is formulated. Section III considers the case where sound waves in these two media can be scattered at large angles. In Sec. IV, the narrow-angle approximation for sound propagation in a forest and turbulent atmosphere is studied. The effect of sound scattering on the interference between the direct and ground-reflected waves is analyzed in Sec. V. Conclusions are summarized in Sec. VI.

II. CORRESPONDENCE BETWEEN SOUND PROPAGATION IN A FOREST AND TURBULENT ATMOSPHERE

Sound propagation in an inhomogeneous, non-turbulent atmosphere is affected by several factors such as refraction, diffraction, and interaction with the ground. These factors can be accounted for with the well-known equations such as a Helmholtz equation or parabolic equation (PE) with the corresponding boundary conditions at the ground. In addition to these factors, a forest and atmospheric turbulence result in sound scattering. If this scattering can be described similarly for both media, the equations for the statistical moments of the sound field should have the same form.

A. Cross sections

For both a forest and turbulent atmosphere, the quantities characterizing sound scattering are the DSCS, σ_d, and TCS, σ; see Ref. 2 and Sec. 6.4 in Ref. 14. The DSCS is defined as follows:

$$\sigma_d(\mathbf{R}_c;\mathbf{n}',\mathbf{n}) = \frac{I_s(\mathbf{R}_c;\mathbf{n}',\mathbf{n})R^2}{I_0 V}. \tag{1}$$

Here, V is the scattering volume, which contains random inhomogeneities, $\mathbf{R}_c$ are the coordinates of its center, R is the distance between $\mathbf{R}_c$ and the receiver, I_0 is the intensity of a plane sound wave incident on the scattering volume, I_s is the intensity of the scattered wave at the receiver, and $\mathbf{n}$ and $\mathbf{n}'$ are the unit vectors in the directions of the incident and scattered waves, respectively (Fig. 1).

The TCS is a sum of the absorption cross section (ACS), σ_a, and the scattering cross section (SCS), σ_s,

$$\sigma(\mathbf{R}_c;\mathbf{n}) = \sigma_a(\mathbf{R}_c;\mathbf{n}) + \sigma_s(\mathbf{R}_c;\mathbf{n}). \tag{2}$$

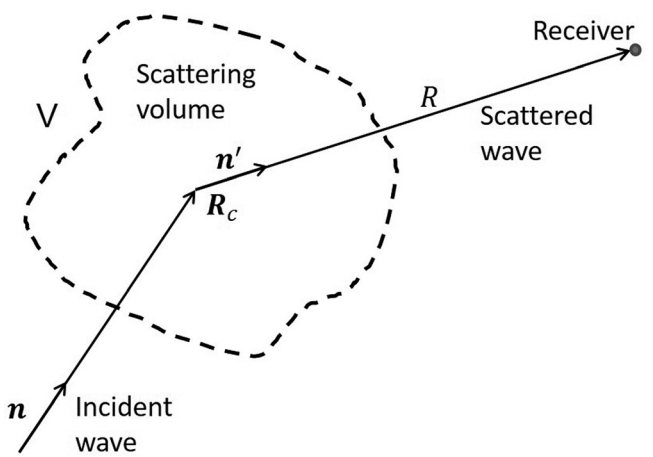

FIG. 1. Geometry for determining the DSCS. V is the scattering volume, $\mathbf{R}_c$ is its center, and $\mathbf{n}$ and $\mathbf{n}'$ are the unit vectors in the directions of the incident and scattered waves, respectively.

These cross sections depend on the direction of sound propagation $\mathbf{n}$. The ACS characterizes acoustic energy absorbed during scattering. The SCS characterizes the loss of energy due to sound scattering in all directions and can be expressed in terms of the DSCS,

$$\sigma_s(\mathbf{R}_c;\mathbf{n}) = \int_{4\pi} \sigma_d(\mathbf{R}_c;\mathbf{n}',\mathbf{n})\, d\Omega(\mathbf{n}'). \tag{3}$$

Here $d\Omega(\mathbf{n}') = \sin\theta' d\theta' d\varphi'$ is the solid angle in the direction of the unit vector $\mathbf{n}'$, where θ' and φ' are the polar and azimuthal angles of $\mathbf{n}'$, respectively, in a spherical coordinate system. If $\sigma_a = 0$, then $\sigma = \sigma_s$ and only the DSCS is needed to completely describe sound scattering.

The mean sound field in a random medium can be calculated as that in a non-random medium if the sound wavenumber k is replaced with the effective wavenumber $k_{\text{eff}} = k_1 + i\gamma$. Here, k_1 and γ are the real and imaginary parts of the effective wavenumber, respectively, with γ being termed as the extinction coefficient of the mean sound field. There is a useful relationship between the TCS and the effective sound wavenumber,

$$\sigma = 2\,\mathrm{Im}\, k_{\text{eff}} = 2\gamma. \tag{4}$$

This relationship is a consequence of the optical theorem.

If the equations for the statistical moments of the sound field propagating in a forest and turbulent atmosphere are expressed in terms of σ_d and σ, these equations should have the same form. This similarity can be found in Refs. 12 and 13, and is also demonstrated below by several examples. In the present paper, this similarity is used to advance formulations of sound propagation in a forest using results known for a turbulent atmosphere and vice versa. Although the equations for the statistical moments of the sound field in a forest and turbulent atmosphere can be expressed in the same form, σ_d and σ in these equations are quite different in these two media. Below we specify the cross sections in a turbulent atmosphere and forest.

B. Turbulent atmosphere

In a turbulent atmosphere, the DSCS may be given by [e.g., Eq. (6.114) in Ref. 14],

$$\sigma_d(\mathbf{R}_c;\mathbf{n}',\mathbf{n}) = 2\pi k^4 \left[\frac{(\mathbf{n}'\cdot\mathbf{n})\Phi_T(\mathbf{R}_c; k(\mathbf{n}-\mathbf{n}'))}{4T_0^2} + \frac{(\mathbf{n}'\cdot\mathbf{n})^2 n_i n_j \Phi_{ij}(\mathbf{R}_c; k(\mathbf{n}-\mathbf{n}'))}{c_0^2} \right], \tag{5}$$

where Φ_T is the spectrum of temperature fluctuations, Φ_{ij} is the spectral tensor of wind velocity fluctuations, and T_0 and c_0 are the reference values of temperature and sound speed, respectively. For sound scattering by atmospheric turbulence, $\sigma_a = 0$ so that $\sigma = \sigma_s$. Substituting σ_d into Eq. (3), we can calculate the TCS, σ, and the extinction coefficient, γ, for different spectra of turbulence.

C. Forest

A forest consists of discrete scatterers such as trunks, branches, and the canopy. Scattering by one scatterer is characterized by the scattering amplitude $f(\mathbf{R}_c;\mathbf{n}',\mathbf{n})$ defined as follows. Suppose that a plane sound wave propagating in the direction of the vector $\mathbf{n}$ is incident on a scatterer centered at $\mathbf{R}_c$ (Fig. 2). In the far field, the sound pressure of the scattered field can be expressed in terms of the scattering amplitude,

$$p_s(\mathbf{R}) = p_0 f(\mathbf{R}_c;\mathbf{n}',\mathbf{n}) \frac{\exp(ik|\mathbf{R}-\mathbf{R}_c|)}{|\mathbf{R}-\mathbf{R}_c|}. \tag{6}$$

Here, p_0 is the amplitude of the incident plane wave and $\mathbf{n}'$ is the unit vector in the direction to the observation point $\mathbf{R}$. Using this formula, the intensity I_s of the scattered sound field can be calculated. Substituting the result into Eq. (1) and replacing $1/V$ with the number of scatterers per unit volume ν, we obtain the DSCS for discrete scatterers

$$\sigma_d(\mathbf{R}_c;\mathbf{n}',\mathbf{n}) = \nu |f(\mathbf{R}_c;\mathbf{n}',\mathbf{n})|^2. \tag{7}$$

The TCS and SCS can be calculated with Eqs. (2) and (3), respectively. However, in many cases, it is more convenient to calculate the TCS using the optical theorem,

$$\sigma(\mathbf{R}_c;\mathbf{n}) = \frac{4\pi\nu}{k}\,\mathrm{Im} f(\mathbf{R}_c;\mathbf{n},\mathbf{n}). \tag{8}$$

Here, $f(\mathbf{R}_c;\mathbf{n},\mathbf{n})$ is the forward scattering amplitude.

Reference 2 provides the DSCS for trunks, branches, and the canopy. The trunks and branches are modeled as vertical and slanted finite solid cylinders, while the canopy layer is modeled with diffuse scatterers. For concreteness, we will consider sound scattering by trunks. The scattering amplitude of a finite cylinder is obtained in Ref. 23. Substituting the result into Eq. (7), we obtain the DSCS

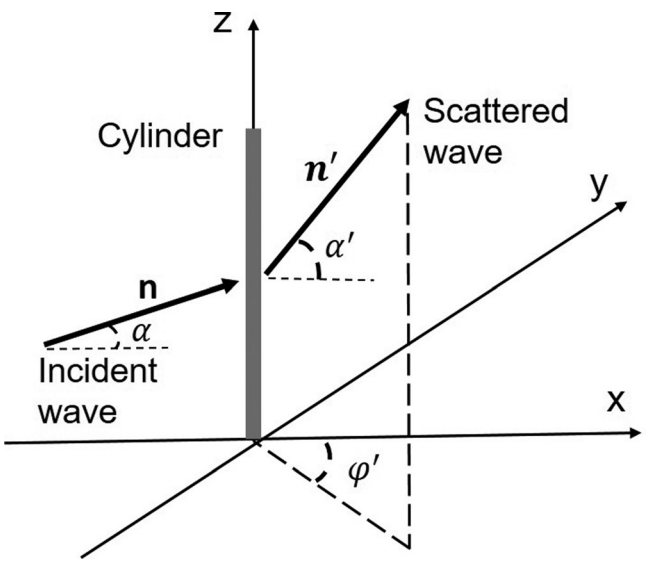

FIG. 2. Geometry for determining the scattering amplitude of a discrete scatterer. The unit vectors $\mathbf{n}$ and $\mathbf{n}'$ are in the directions of the incident and scattered waves, respectively.

$$\sigma_d(\mathbf{n}',\mathbf{n}) = \sigma_d(\alpha',\varphi';\alpha,\varphi) = \nu k^2 h^2 b^2 \,\mathrm{sinc}^2\left[kh(\sin\alpha' - \sin\alpha)/2\right] \times \left|\sum_{n=0}^{\infty} B_n \cos\left[n(\varphi' - \varphi)\right]\right|^2. \quad (9)$$

Here b is the radius of the cylinder, h is its height, $\mathrm{sinc}(\eta) = \sin(\eta)/\eta$ is the sinc function, and the unit vector $\mathbf{n}'$ is expressed as

$$\mathbf{n}' = (n_x', n_y', n_z') = (\cos\alpha'\cos\varphi', \cos\alpha'\sin\varphi', \sin\alpha'). \quad (10)$$

Here α' is the angle between $\mathbf{n}'$ and the plane perpendicular to the axis of the cylinder and φ' is the azimuthal angle (Fig. 2). These angles vary within the intervals $[-\pi/2,\pi/2]$ and $[-\pi,\pi]$, respectively. The angles α and φ pertinent to the unit vector $\mathbf{n}$ are defined similarly. The functions B_n are

$$B_n(\alpha',\alpha) = \frac{\varepsilon_n}{2} J'_n(kb\cos\alpha)\left[\cos\alpha J_n(kb\cos\alpha') - \cos\alpha' J'_n(kb\cos\alpha')\frac{H_n^{(1)}(kb\cos\alpha)}{H_n^{(1)\prime}(kb\cos\alpha)}\right], \quad (11)$$

where J_n is the Bessel function, $H_n^{(1)}$ is the Hankel function of the first kind, primes above J_n and $H_n^{(1)}$ denote derivatives with respect to the argument, and ε_n is the Neumann factor: $\varepsilon_0 = 1$ and $\varepsilon_n = 2$ for $n \neq 0$.

For sound scattering by solid cylinders, $\sigma_a = 0$ so that $\sigma = \sigma_s$. The TCS is obtained with the use of Eq. (8),[2]

$$\sigma(\alpha) = \frac{4\nu h}{k}\mathrm{Re}\sum_{n=0}^{\infty}\varepsilon_n \frac{J'_n(kb\cos\alpha)}{H_n^{(1)\prime}(kb\cos\alpha)}. \quad (12)$$

III. WIDE-ANGLE SCATTERING

When considering sound propagation in a forest and turbulent atmosphere, it useful to treat separately two cases. In the first case considered in this section, a sound wave can be scattered at wide (or all) angles. Wide-angle scattering occurs if the sound wavelength λ is greater than the scale L of discrete scatterers or medium inhomogeneities. In this case, using 3D multiple scattering theory, calculation of the correlation function of the sound field both in a forest and turbulent atmosphere can be reduced to the RTE. In the second case (Sec. IV), a sound wave is scattered predominantly in the direction of propagation.

A. Forest

For sound propagation in a forest, the starting equations are the Helmholtz equation in free space and the sound field scattered by a discrete scatterer. Assuming that there are many scatterers whose positions are random, an integral equation for the spatial correlation function of the sound field $p(\mathbf{R})$ can be derived.[12,13] This correlation function can be expressed in terms of the radiance $J(\mathbf{R}_c,\mathbf{n})$,

$$B(\mathbf{R}_c,\mathbf{R}_d) = \langle p(\mathbf{R}_1)p^*(\mathbf{R}_2)\rangle = \varrho c_0 \int_{4\pi} J(\mathbf{R}_c,\mathbf{n}) e^{ik_1\mathbf{n}\cdot\mathbf{R}_d}\, d\Omega(\mathbf{n}). \quad (13)$$

Here, ϱ is the air density, and $\mathbf{R}_c = (\mathbf{R}_1 + \mathbf{R}_2)/2$ and $\mathbf{R}_d = \mathbf{R}_1 - \mathbf{R}_2$ are the center and difference coordinates, respectively, of the two points of observation, $\mathbf{R}_1$ and $\mathbf{R}_2$. The radiance satisfies the RTE, which can be derived from the integral equation for the correlation function,

$$\left(\mathbf{n}\cdot\frac{\partial}{\partial\mathbf{R}_c}\right)J(\mathbf{R}_c,\mathbf{n}) + \sigma(\mathbf{R}_c;\mathbf{n})J(\mathbf{R}_c,\mathbf{n}) = \int_{4\pi}\sigma_d(\mathbf{R}_c;\mathbf{n},\mathbf{n}')J(\mathbf{R}_c,\mathbf{n}')\,d\Omega(\mathbf{n}') + Q_s(\mathbf{R}_c), \quad (14)$$

where the function $Q_s(\mathbf{R}_c)$ characterizes the sound sources distribution. Reference 2 outlines application of the RTE to forest acoustics. The RTE accounts for sound scattering and absorption by different scatterers in a forest such as trunks, branches, and the canopy. The RTE can be generalized to account for sound refraction.[13]

The radiance J can be written as a sum

$$J(\mathbf{R}_c,\mathbf{n}) = J_{\mathrm{coh}}(\mathbf{R}_c,\mathbf{n}) + J_d(\mathbf{R}_c,\mathbf{n}), \quad (15)$$

where J_{coh} and J_d are the coherent and diffuse radiances, respectively. The J_{coh} satisfies Eq. (14) with $\sigma_d = 0$ and in many cases can be calculated analytically. The diffuse radiance satisfies the integro-differential equation,

$$\left(\mathbf{n}\cdot\frac{\partial}{\partial\mathbf{R}_c}\right)J_d(\mathbf{R}_c,\mathbf{n}) + \sigma(\mathbf{R}_c;\mathbf{n})J_d(\mathbf{R}_c,\mathbf{n}) = \int_{4\pi}\sigma_d(\mathbf{R}_c;\mathbf{n},\mathbf{n}')[J_{\mathrm{coh}}(\mathbf{R}_c,\mathbf{n}') + J_d(\mathbf{R}_c,\mathbf{n}')]\,d\Omega(\mathbf{n}'). \quad (16)$$

Numerical solutions of the RTE are well developed in many fields such as nuclear physics, optics, and radiation transfer in the Earth, planetary, and solar atmospheres (e.g., Sec. 4.6 in Ref. 13 and Ref. 24).

B. Turbulent atmosphere

The starting equation for sound propagation in a turbulent atmosphere is a Helmholtz-type equation [e.g., Eq. (8.53) in Ref. 14], which accounts for scattering by temperature and wind velocity fluctuations and differs significantly from the starting equations for forest acoustics. The correlation function of the sound field in a turbulent atmosphere can also be expressed in terms of the radiance, which satisfies a RTE. Equation (8.107) in Ref. 14 for the diffuse radiance J_d obtained for a homogeneous turbulence (the cross sections do not depend on $\mathbf{R}_c$) coincides with Eq. (16). Thus, even though the starting equations for sound propagation in a forest and turbulent atmosphere are different, the equations for the correlation function of the sound field have the same form.

Using this similarity, we can account for inhomogeneity of atmospheric turbulence in formulations for the correlation

function of the sound field. This correlation function can be written as Eq. (13), in which the radiance $J(\mathbf{R}_c, \mathbf{n})$ satisfies Eq. (14), where the DSCS is given by Eq. (5). This is a new result for sound propagation in a statistically inhomogeneous and anisotropic turbulence, which would be otherwise difficult to obtain.

IV. NARROW-ANGLE APPROXIMATION

Sound propagation in a forest and turbulent atmosphere are usually studied in the narrow-angle approximation using a PE. For sound propagation in a continuous random medium, this approximation is valid if the sound wavelength λ is smaller than the scale L of medium inhomogeneities. (For sound propagation in the atmosphere, L can be chosen as the outer scale of turbulence, e.g., see Secs. 6.2 and 7.1.1 in Ref. 14.) For forest acoustics, a similar requirement is a necessary but not sufficient condition since a solid object scatters sound both in the forward and backward directions. The RTE is applicable for any ratio between λ and L, but significantly simplifies if $\lambda \ll L$. In this section, following Refs. 13 and 25 and using the narrow-angle approximation, the RTE is reduced to the second-moment PE. The cross sections pertinent to sound scattering in a forest and turbulent atmosphere are simplified in this approximation.

A. Second-moment PE

Let us consider sound propagation close to the x axis and assume that the two points of observation, $\mathbf{R}_1 = (x, \mathbf{r}_1)$ and $\mathbf{R}_2 = (x, \mathbf{r}_2)$, be located at the same range x (Fig. 3). In this case, $\mathbf{R}_c = (x, \mathbf{r}_c)$ and $\mathbf{R}_d = (0, \mathbf{r}_d)$, where $\mathbf{r}_c = (\mathbf{r}_1 + \mathbf{r}_2)/2$ and $\mathbf{r}_d = \mathbf{r}_1 - \mathbf{r}_2$ are the center and difference coordinates, respectively, in the plane perpendicular to the x axis.

In the narrow-angle approximation, we have

$$\mathbf{n} = (n_x, \mathbf{n}_\perp) \approx (1 - n_\perp^2/2, \mathbf{n}_\perp) \approx (1, \mathbf{n}_\perp), \tag{17}$$

where $\mathbf{n}_\perp = (n_y, n_z)$ is the component of the vector $\mathbf{n}$ perpendicular to the x axis. In the narrow-angle approximation, $n_\perp$ is a small parameter; hereinafter, all calculations are done to order $n_\perp$. The radiance can be written as

$$J(\mathbf{R}_c, \mathbf{n}) = J(x, \mathbf{r}_c; n_x, \mathbf{n}_\perp) \approx J(x, \mathbf{r}_c; 1, \mathbf{n}_\perp) \equiv J(x, \mathbf{r}_c; \mathbf{n}_\perp). \tag{18}$$

Similarly, we express the cross sections,

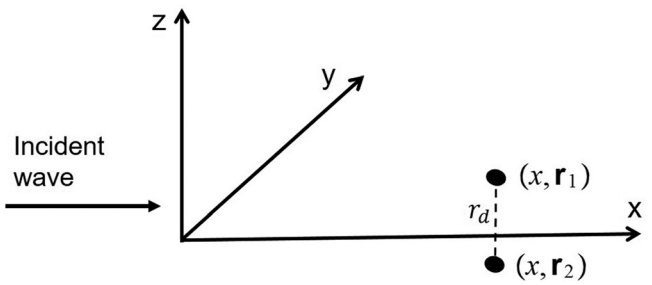

FIG. 3. Schematics of sound propagation in the narrow-angle approximation. The two points of observation, $(x,\mathbf{r}_1)$ and $(x,\mathbf{r}_2)$, are located close to the x axis; r_d is the distance between these points.

$$\sigma(\mathbf{R}_c, \mathbf{n}) \approx \sigma(x, \mathbf{r}_c; 1, \mathbf{n}_\perp) \equiv \sigma(x, \mathbf{r}_c; \mathbf{n}_\perp),$$
$$\sigma_d(\mathbf{R}_c, \mathbf{n}', \mathbf{n}) \approx \sigma_d(x, \mathbf{r}_c; 1, \mathbf{n}'_\perp; 1, \mathbf{n}_\perp) \equiv \sigma_d(x, \mathbf{r}_c; \mathbf{n}'_\perp, \mathbf{n}_\perp). \tag{19}$$

Finally, the differential and integral operators appearing in the RTE simplify,

$$\mathbf{n} \cdot \frac{\partial}{\partial \mathbf{R}_c} = n_x \frac{\partial}{\partial x} + \mathbf{n}_\perp \cdot \frac{\partial}{\partial \mathbf{r}_c} \approx \frac{\partial}{\partial x} + \mathbf{n}_\perp \cdot \frac{\partial}{\partial \mathbf{r}_c},$$
$$\int_{4\pi} d\Omega(\mathbf{n}') \approx \int d^2 n'_\perp \equiv \int dn'_y \int dn'_z. \tag{20}$$

Hereinafter, if the limits of integration are not indicated, they are assumed to be from $-\infty$ to ∞. As a result of these approximations, the RTE, Eq. (14), takes the form

$$\left[\frac{\partial}{\partial x} + \mathbf{n}_\perp \cdot \frac{\partial}{\partial \mathbf{r}_c} + \sigma(x, \mathbf{r}_c; \mathbf{n}_\perp)\right] J(x, \mathbf{r}_c; \mathbf{n}_\perp) = \int \sigma_d(x, \mathbf{r}_c; \mathbf{n}_\perp, \mathbf{n}'_\perp) J(x, \mathbf{r}_c; \mathbf{n}'_\perp)\, d^2 n'_\perp. \tag{21}$$

In Eq. (13), we assume for simplicity that $k_1 = k$. We also express $\mathbf{n}_\perp = \boldsymbol{\kappa}_\perp/k$, where $\boldsymbol{\kappa}_\perp = (\kappa_y, \kappa_z)$ is a vector in the plane perpendicular to the x axis, and write $J(x, \mathbf{r}_c; \mathbf{n}_\perp) \equiv J(x, \mathbf{r}_c; \boldsymbol{\kappa}_\perp/k)$ as $J(x, \mathbf{r}_c; \boldsymbol{\kappa}_\perp)$. Then, Eq. (13) becomes

$$B(x; \mathbf{r}_c, \mathbf{r}_d) = \frac{\varrho c_0}{k^2} \int J(x, \mathbf{r}_c; \boldsymbol{\kappa}_\perp) e^{i\boldsymbol{\kappa}_\perp \cdot \mathbf{r}_d}\, d^2 \kappa_\perp. \tag{22}$$

With these notations, Eq. (21) takes the form

$$\left[\frac{\partial}{\partial x} + \frac{\boldsymbol{\kappa}_\perp}{k} \cdot \frac{\partial}{\partial \mathbf{r}_c} + \sigma(x, \mathbf{r}_c; \boldsymbol{\kappa}_\perp/k)\right] J(x, \mathbf{r}_c; \boldsymbol{\kappa}_\perp) = \frac{1}{k^2} \int \sigma_d(x, \mathbf{r}_c; \boldsymbol{\kappa}_\perp/k, \boldsymbol{\kappa}'_\perp/k) J(x, \mathbf{r}_c; \boldsymbol{\kappa}'_\perp)\, d^2 \kappa'_\perp. \tag{23}$$

As will be shown below, for sound propagation in a forest and turbulent atmosphere the TCS and DSCS can be written as

$$\sigma(x, \mathbf{r}_c; \boldsymbol{\kappa}_\perp/k) \approx \sigma(x, \mathbf{r}_c), \quad \sigma_d(x, \mathbf{r}_c; \boldsymbol{\kappa}_\perp/k, \boldsymbol{\kappa}'_\perp/k) \approx \sigma_d(x, \mathbf{r}_c; (\boldsymbol{\kappa}_\perp - \boldsymbol{\kappa}'_\perp)/k). \tag{24}$$

We apply the operator $(1/k^2) \int \exp(i\boldsymbol{\kappa}_\perp \cdot \mathbf{r}_d)\, d^2 \kappa_\perp$ to both sides of Eq. (23). After some manipulations and taking into account Eqs. (22) and (24), we obtain a differential equation for the correlation function of the sound field

$$\left[\frac{\partial}{\partial x} - \frac{i}{k} \frac{\partial^2}{\partial \mathbf{r}_c \partial \mathbf{r}_d} + \sigma(x, \mathbf{r}_c)\right] B(x; \mathbf{r}_c, \mathbf{r}_d) = B(x; \mathbf{r}_c, \mathbf{r}_d) \frac{1}{k^2} \int \sigma_d(x, \mathbf{r}_c; \boldsymbol{\kappa}_\perp/k) e^{i\boldsymbol{\kappa}_\perp \cdot \mathbf{r}_d}\, d^2 \kappa_\perp. \tag{25}$$

In this equation, we recall that $\sigma = \sigma_a + \sigma_s$. In the narrow-angle approximation, σ_s can be written as

$$\sigma_s(x, \mathbf{r}_c) = \frac{1}{k^2} \int \sigma_d(x, \mathbf{r}_c; \boldsymbol{\kappa}_\perp/k)\, d^2 \kappa_\perp. \tag{26}$$

Using this formula, we obtain the desired form of a differential equation for the correlation function,

$$\left[\frac{\partial}{\partial x}-\frac{i}{k}\frac{\partial^2}{\partial \mathbf{r}_c \partial \mathbf{r}_d}+\sigma_a(x,\mathbf{r}_c)+Q(x;\mathbf{r}_c,\mathbf{r}_d)\right]B(x;\mathbf{r}_c,\mathbf{r}_d)=0. \tag{27}$$

Here,

$$Q(x;\mathbf{r}_c,\mathbf{r}_d)=\frac{1}{k^2}\int \sigma_d(x,\mathbf{r}_c;\boldsymbol{\kappa}_\perp/k)(1-e^{i\boldsymbol{\kappa}_\perp\cdot\mathbf{r}_d})\,d^2\kappa_\perp. \tag{28}$$

Thus, in the narrow-angle approximation, the RTE reduces to Eq. (27). This a parabolic-type equation for the correlation function of the sound field, $B(x;\mathbf{r}_c,\mathbf{r}_d)$, and we refer to this equation as the second-moment PE. This equation is valid for sound propagation in a statistically inhomogeneous and anisotropic random medium (discrete or continuous). Equation (27) is much simpler than the RTE and can be readily solved numerically. If the approximation $k_1=k$ is not used, the correlation function still satisfies Eqs. (27) and (28) with k replaced by k_1.

The results obtained in this subsection are valid for arbitrary cross sections. In Secs. IV B and IV C, we specify the DSCS in a turbulent atmosphere and the trunk region of a forest. Equation (27) is a new result in forest acoustics; in atmospheric acoustics, this equation has been previously used for analytical and numerical calculations (Secs. 7.4.4 and 11.2.3 in Ref. 14 and Refs. 26–28).

B. Turbulent atmosphere

In Eq. (5), we ignore terms proportional to $n_\perp^2$ and also omit products of two small quantities such as $n_\perp\Phi_{12}$ (this term is small in comparison with $\Phi_{11}\equiv\Phi_{xx}$). As a result, in the narrow-angle approximation, the DSCS in a turbulent atmosphere simplifies,

$$\sigma_d(x,\mathbf{r}_c;\mathbf{n}'_\perp-\mathbf{n}_\perp)=\frac{\pi k^4}{2}\left[\frac{\Phi_T(x,\mathbf{r}_c;0,k(\mathbf{n}_\perp-\mathbf{n}'_\perp))}{T_0^2}+\frac{4\Phi_{11}(x,\mathbf{r}_c;0,k(\mathbf{n}_\perp-\mathbf{n}'_\perp))}{c_0^2}\right]. \tag{29}$$

In this formula, the quantity in the square brackets can be recognized as the effective spectrum of turbulence,

$$\Phi_{\text{eff}}(x,\mathbf{r}_c;0,\boldsymbol{\kappa}_\perp)=\frac{\Phi_T(x,\mathbf{r}_c;0,\boldsymbol{\kappa}_\perp)}{T_0^2}+\frac{4\Phi_{11}(x,\mathbf{r}_c;0,\boldsymbol{\kappa}_\perp)}{c_0^2}, \tag{30}$$

where $\boldsymbol{\kappa}_\perp=k(\mathbf{n}_\perp-n'_\perp)$. With these notations, Eq. (29) can be written as

$$\sigma_d(x,\mathbf{r}_c;\boldsymbol{\kappa}_\perp/k)=\frac{\pi k^4}{2}\Phi_{\text{eff}}(x,\mathbf{r}_c;0,\boldsymbol{\kappa}_\perp). \tag{31}$$

This formula relates the DSCS pertinent to the RTE with the effective spectrum Φ_{eff}, which plays a key role in the theories of sound propagation in a turbulent atmosphere in the PE approximation (Chap. 7 in Ref. 14).

Substituting Eq. (31) into Eq. (26), the TCS and SCS are expressed in terms of the effective spectrum,

$$\sigma(x,\mathbf{r}_c)\equiv\sigma_s(x,\mathbf{r}_c)=\frac{\pi k^2}{2}\int\Phi_{\text{eff}}(x,\mathbf{r}_c;0,\boldsymbol{\kappa}_\perp)\,d^2\kappa_\perp. \tag{32}$$

Substituting Eq. (31) into Eq. (28), we express the function Q via the effective spectrum,

$$Q(x;\mathbf{r}_c,\mathbf{r}_d)=\frac{\pi k^2}{2}\int\Phi_{\text{eff}}(x,\mathbf{r}_c;0,\boldsymbol{\kappa}_\perp)(1-e^{i\boldsymbol{\kappa}_\perp\cdot\mathbf{r}_d})\,d^2\kappa_\perp. \tag{33}$$

The first two statistical moments of the sound field in the turbulent atmosphere in the PE approximation are analyzed in Chap. 7 of Ref. 14. It is insightful to compare these statistical moments with those obtained above by considering the RTE and cross sections in the narrow-angle approximation. The extinction coefficient of the mean sound field $\gamma=\sigma_s/2$, which can be obtained with Eqs. (4) and (32), coincides with Eq. (7.151) in Ref. 14. The second-moment PE for the correlation function, Eq. (27) with $\sigma_a=0$ and Q given by Eq. (33), coincides with Eq. (7.158) in this reference. This correspondence elucidates the connection between the RTE in the narrow-angle approximation and the PE approximation.

C. Forest

For sound propagation in a forest in the narrow-angle approximation, the TCS is still given by Eq. (12), where $\alpha=0$. In this formula, in the considered high-frequency approximation, the real part of the infinite series tends to kb. As a result, the TCS becomes

$$\sigma(\alpha=0)=4\nu hb=2\nu S_p. \tag{34}$$

Here $S_p=2hb$ is the projected area of one cylinder. This result, as it should, coincides with the high-frequency approximation for the TCS for solid objects (e.g., Sec. 9.1 in Ref. 29). In this approximation, half of the energy is scattered in the narrow cone in the direction of sound propagation and the other half in other directions (e.g., Sec. 8.1 in Ref. 30). Therefore, the TCS can be written as $\sigma=\sigma_f+\sigma_o$, where σ_f and σ_o are the TCSs in the forward and other directions,

$$\sigma_f=\sigma_o=2\nu hb. \tag{35}$$

In the considered approximation, the angles α, α', φ, and φ' appearing in Eq. (9) for the DSCS are small. From Eq. (10), we have $\mathbf{n}'\approx(1,n'_y,n'_z)=(1,\varphi',\alpha')$. The vector $\mathbf{n}$ can be approximated similarly. As a result, Eq. (9) simplifies,

$$\sigma_d(\mathbf{n}'_\perp-\mathbf{n}_\perp)=\nu k^2h^2b^2\,\text{sinc}^2\left[kh(n'_z-n_z)/2\right]\times\left|\sum_{n=0}^{\infty}B_n\cos\left[n(n'_y-n_y)\right]\right|^2. \tag{36}$$

Introducing the vector $\boldsymbol{\kappa}_\perp \equiv (\kappa_y, \kappa_z) = k(\mathbf{n}'_\perp - \mathbf{n}_\perp)$, we have

$$\sigma_d(\boldsymbol{\kappa}_\perp) = \nu k^2 h^2 b^2 \,\mathrm{sinc}^2(h\kappa_z/2)\left|\sum_{n=0}^{\infty} B_n \cos(n\kappa_y/k)\right|^2. \tag{37}$$

In this formula, the functions B_n given by Eq. (11) can be evaluated at $\alpha = \alpha' = 0$,

$$B_n(0,0) = \frac{i\varepsilon_n}{\pi kb}\frac{J'_n(kb)}{H_n^{(1)\prime}(kb)}. \tag{38}$$

The forward TCS, σ_f, can also be calculated by substituting $\sigma_d(\boldsymbol{\kappa}_\perp)$ into Eq. (26). The integration over κ_z can be reduced to evaluation of the integral $\int_0^\infty \mathrm{sinc}^2(\eta)\,d\eta$, which is equal to $\pi/2$. In the integral over κ_y, we introduce a new variable $\varphi = \kappa_y/k$. With these manipulations, we obtain

$$\sigma_f = \frac{2\nu h}{\pi k} I_\varphi. \tag{39}$$

Here, the integral I_φ is given by

$$I_\varphi = \int_{-\infty}^{\infty} \sum_{n,m=0}^{\infty} \varepsilon_n \varepsilon_m \cos(n\varphi)\cos(m\varphi) \times \frac{J'_n(kb)J'_m(kb)}{H_n^{(1)\prime}(kb)\left(H_m^{(1)\prime}(kb)\right)^*}\,d\varphi. \tag{40}$$

The value of $I_\varphi = \pi kb$ can be obtained by taking into account that σ_f is given by Eq. (35) in the considered approximation.

D. Sound propagation above an impedance ground in a refractive, turbulent atmosphere

In many cases, sound propagation in a turbulent atmosphere and forest should account for sound refraction and interaction with the impedance ground. For a turbulent atmosphere, Sec. 8.2.4 in Ref. 14 generalizes Eq. (27) for these phenomena. The correlation function of the sound field $B(x;\mathbf{r}_1,\mathbf{r}_2) = \langle p(x,\mathbf{r}_1)p^*(x,\mathbf{r}_2)\rangle$ satisfies the following equation:

$$\left[\frac{\partial}{\partial x} - \frac{i}{2k}\hat{M} + Q(x;\mathbf{r}_1,\mathbf{r}_2)\right]B(x;\mathbf{r}_1,\mathbf{r}_2) = 0. \tag{41}$$

Here, the operator $\hat{M}$ is given by

$$\hat{M} = \nabla^2_{\mathbf{r}_1} - \nabla^2_{\mathbf{r}_2} + k^2\left[\frac{c_0^2}{c_{\mathrm{eff}}^2(x,\mathbf{r}_1)} - \frac{c_0^2}{c_{\mathrm{eff}}^2(x,\mathbf{r}_2)}\right] + \frac{2ik}{c_0}\left[\mathbf{v}_\perp(x,\mathbf{r}_1)\cdot\nabla_{\mathbf{r}_1} + \mathbf{v}_\perp(x,\mathbf{r}_2)\cdot\nabla_{\mathbf{r}_2}\right], \tag{42}$$

where $\nabla_{\mathbf{r}_1} = (\partial/\partial y_1, \partial/\partial z_1)$ and similarly for $\nabla_{\mathbf{r}_2}$, $c_{\mathrm{eff}} = c + v_x$ is the effective sound speed, c is the sound speed, and v_x and $\mathbf{v}_\perp$ are the components of the wind velocity along the x axis and perpendicular to it. The third and fourth terms in the operator $\hat{M}$ describe refraction and advection of sound with the cross wind, respectively. In Eq. (41), the function Q is given by

$$Q(x;\mathbf{r}_1,\mathbf{r}_2) = \frac{\pi k^2}{4}\int[\Phi_{\mathrm{eff}}(x,\mathbf{r}_1;0,\boldsymbol{\kappa}_\perp) + \Phi_{\mathrm{eff}}(x,\mathbf{r}_2;0,\boldsymbol{\kappa}_\perp) - 2e^{i\boldsymbol{\kappa}_\perp\cdot(\mathbf{r}_1-\mathbf{r}_2)} \times \Phi_{\mathrm{eff}}\left(x,(\mathbf{r}_1+\mathbf{r}_2)/2;0,\boldsymbol{\kappa}_\perp\right)]\,d^2\kappa_\perp. \tag{43}$$

For a quasi-homogeneous turbulence, the effective spectrum $\Phi_{\mathrm{eff}}(x,\mathbf{r}_1;0,\boldsymbol{\kappa}_\perp)$ is a slow varying function with respect to $(x, \mathbf{r}_1)$. Therefore, we can approximate the effective spectrum as $\Phi_{\mathrm{eff}}(x,(\mathbf{r}_1+\mathbf{r}_2)/2;0,\boldsymbol{\kappa}_\perp)$. The effective spectrum $\Phi_{\mathrm{eff}}(x,\mathbf{r}_2;0,\boldsymbol{\kappa}_\perp)$ can be approximated similarly. Substituting these results into Eq. (43) and expressing $\Phi_{\mathrm{eff}}(x,(\mathbf{r}_1+\mathbf{r}_2)/2;0,\boldsymbol{\kappa}_\perp)$ in terms of the DSCS, we obtain

$$Q(x;\mathbf{r}_1,\mathbf{r}_2) = \frac{1}{k^2}\int\sigma_d\left(x,(\mathbf{r}_1+\mathbf{r}_2)/2;0,\boldsymbol{\kappa}_\perp\right) \times\left[1 - e^{i\boldsymbol{\kappa}_\perp\cdot(\mathbf{r}_1-\mathbf{r}_2)}\right]d^2\kappa_\perp. \tag{44}$$

This formula coincides with Eq. (28) if $\mathbf{r}_1$ and $\mathbf{r}_2$ are expressed in terms of $\mathbf{r}_c$ and $\mathbf{r}_d$, respectively. It can also be shown that if refraction and advection are absent, Eq. (41) coincides with Eq. (27).

Sound interaction with the ground is accounted for with the impedance boundary conditions,

$$\left.\frac{\partial B(x;y_1,z_1;y_2,z_2)}{\partial z_1}\right|_{z_1=0} = -ik\beta_g B(x;y_1,z_1;y_2,z_2)|_{z_1=0}, \tag{45}$$

$$\left.\frac{\partial B(x;y_1,z_1;y_2,z_2)}{\partial z_2}\right|_{z_2=0} = ik\beta_g^* B(x;y_1,z_1;y_2,z_2)|_{z_2=0}, \tag{46}$$

where β_g is the normalized admittance of the ground. Equation (41) with these boundary conditions has been used to study the correlation function of the sound field and mean intensity propagating above the impedance ground in a refractive turbulent atmosphere.[14,26,28]

E. Sound propagation above an impedance ground in a forest with micrometeorology

Equation (41) can also be used in forest acoustics, where it is often important to account for atmospheric stratification due to micrometeorology.[31]

For sound propagation in a forest, the term $\sigma_a(x, \mathbf{r}_c)$ should be included in the square brackets in Eq. (41) to account for possible sound absorption,

$$\left[\frac{\partial}{\partial x} - \frac{i}{2k}\hat{M} + \sigma_a(x,\mathbf{r}_c) + Q(x;\mathbf{r}_1,\mathbf{r}_2)\right]B(x;\mathbf{r}_1,\mathbf{r}_2) = 0. \tag{47}$$

This equation and the boundary conditions, Eqs. (45) and (46), describe sound propagation above an impedance ground

in a forest with temperature and wind velocity stratification. Effective solutions of Eq. (47) have been developed for sound propagation in a turbulent atmosphere (Sec. 11.2.3 in Ref. 14 and Refs. 26–28) and can be used in forest acoustics. Formulation of this equation is one of the main results of the current paper.

As explained above, when sound propagates through tree trunks, half of the energy is scattered in the direction of propagation and the other half in other directions. To account for the loss of energy due to scattering in other directions, the effective ACS, σ_a^{eff}, can be added into the square brackets in Eq. (47). The effective ACS can be chosen as $\sigma_a^{\text{eff}} = g\sigma_o$, where σ_o is given by Eq. (35) and g is a numerical factor (or adjustable parameter) of order unity.

V. INTERFERENCE BETWEEN DIRECT AND GROUND-REFLECTED WAVES

In the atmosphere at relatively short propagation ranges, the sound field at the receiver is a sum of the direct and ground-reflected waves. The interference between these two waves results in maxima and minima of the sound pressure level (SPL) as a function of frequency. Scattering of sound by atmospheric turbulence and trees diminishes the coherence between the direct and ground-reflected waves, and can significantly change the interference pattern. This phenomenon is well studied for sound scattering by atmospheric turbulence, but remains an important, unsolved problem in forest acoustics. In this section, using the results pertinent to sound propagation in a turbulent atmosphere, the interference of the direct and ground-reflected waves in a forest is considered.

A. Turbulent atmosphere

The geometry of the problem is shown in Fig. 4. The source and receiver coordinates are $\mathbf{R}_s = (0,\ 0,\ h_s)$ and $\mathbf{R}_r = (x,0,h_r)$, respectively. Here, h_s and h_r are the source and receiver heights above the ground and x is the distance between them. The subscripts s and r correspond to the source and receiver, respectively.

The interference of the direct and ground-reflected waves in a turbulent atmosphere is described in detail in Sec. 8.1 of Ref. 14. The mean-squared sound pressure due to a unit strength point source is given by[18,19]

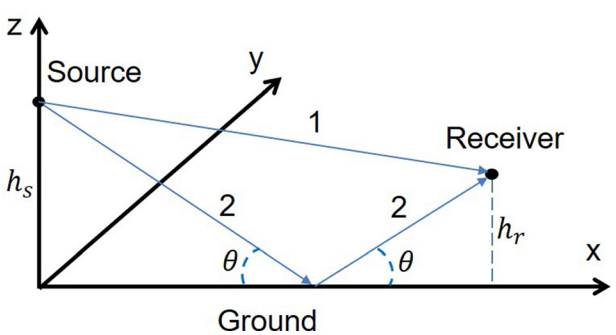

FIG. 4. (Color online) Schematics of the interference of the direct (1) and ground-reflected (2) waves in the atmosphere.

$$\langle pp^* \rangle = \frac{1}{R_1^2} + \frac{|\mathcal{R}|^2}{R_2^2} + \frac{2|\mathcal{R}|C_{\text{coh}}}{R_1 R_2}\cos[k(R_2 - R_1) + \beta]. \tag{48}$$

Here, $R_1 = \sqrt{x^2 + (h_s - h_r)^2}$ and $R_2 = \sqrt{x^2 + (h_s + h_r)^2}$ are the path lengths of the direct and ground-reflected waves, and $\mathcal{R} = |\mathcal{R}|\exp(i\beta)$ is the spherical-wave reflection coefficient. The indices 1 and 2 refer to the direct and ground-reflected waves (Fig. 4). In the approximation of the near-grazing sound propagation ($x \gg h_s,h_r$) and for the locally reacting surface, $\mathcal{R}$ is given by

$$\mathcal{R} = \frac{Z\sin\theta - 1 + 2F(d)}{Z\sin\theta + 1}, \tag{49}$$

where Z is the normalized specific impedance of the ground, θ is the grazing angle of the wave incident on the ground, and

$$F(d) = \left[1 + i\sqrt{\pi}d\,\exp(-d^2)\text{erfc}(-id)\right] \tag{50}$$

is the boundary loss factor. Here, $d = \sqrt{ikR_2/2}(1/Z + \sin\theta)$ is the numerical distance and erfc is the complementary error function.

In Eq. (48), C_{coh} is the coherence factor, which describes the coherence between the direct and ground-reflected waves and is given by [Eq. (8.24) in Ref. 14 and Refs. 20,21]

$$C_{\text{coh}} = \exp\left[-\frac{\pi k^2 x}{2}\int_0^1 d\eta \int \Phi_{\text{eff}}(0,\boldsymbol{\kappa}_\perp)\left(1 - e^{i\eta\kappa_z h_{sr}}\right)d^2\kappa_\perp\right], \tag{51}$$

where $h_{sr} = 2h_s h_r/(h_s + h_r)$ is the maximum separation between the direct path from the source to the receiver and the path reflected from the ground. Expressing the effective spectrum in terms of the DSCS [Eq. (31)], we obtain

$$C_{\text{coh}} = \exp\left[-\frac{x}{k^2}\int_0^1 d\eta \int_{-\infty}^{\infty} d\kappa_y \times \int_{-\infty}^{\infty} d\kappa_z\, \sigma_d(\kappa_y,\kappa_z)\left(1 - e^{i\eta\kappa_z h_{sr}}\right)\right]. \tag{52}$$

These equations have been used to analyze the interference between the direct and ground-reflected waves in a turbulent atmosphere.

B. Forest

Given the similarity between equations for the statistical moments of the sound field in discrete and continuous random media, we argue that the equations in Sec. V A also describe the interference between the direct and ground-reflected waves in a forest. In particular, the mean-squared sound pressure is given by Eq. (48), where the coherence factor is determined with Eq. (52).

Substituting the DSCS in the trunk layer into Eq. (52), we obtain the coherence factor for sound propagation in a forest,

$$C_{\rm coh} = \exp\left[-\nu x h^2 b^2 \int_0^1 d\eta \int_{-\infty}^{\infty} d\kappa_z \times (1 - e^{i\eta\kappa_z h_{sr}}) \mathrm{sinc}^2(\kappa_z h/2) \times \int_{-\infty}^{\infty} d\kappa_y \sum_{n,m=0}^{\infty} B_n B_m^* \cos(n\kappa_y/k) \cos(m\kappa_y/k)\right]. \quad (53)$$

In this formula, the integral over η can be readily evaluated. The integral over κ_y equals $I_\varphi/(\pi^2 k b^2) = 1/(\pi b)$. With these manipulations, we obtain

$$C_{\rm coh} = \exp\left[-x\sigma_f F(h_{sr}/h)\right] = \exp\left[-2x\nu h b F(h_{sr}/h)\right]. \quad (54)$$

Here, σ_f is determined with Eq. (35) and function F is given by

$$F(h_{sr}/h) = \frac{2}{\pi}\int_0^{\infty} [1 - \mathrm{sinc}(2\eta h_{sr}/h)]\mathrm{sinc}^2\eta\, d\eta. \quad (55)$$

It follows from Eq. (54) that the coherence factor decreases exponentially with increasing range x. The attenuation coefficient equals the product of the forward TSC σ_f and function $F(h_{sr}/h)$, which is plotted in Fig. 5. It follows from Fig. 5 that $F(h_{sr}/h)$ monotonically increases with increasing ratio h_{sr}/h. If both the source and receiver are located inside the forest ($h_s \le h$ and $h_r \le h$, respectively), it can be shown that $h_{sr}/h \le \sqrt{2}$. In this case, the maximum value of F is 0.646 (Fig. 5). It also follows from Fig. 5 that $F \approx 0.5 h_{sr}/h$ if $h_{sr}/h \le 1$. In this case, the coherence factor takes the form

$$C_{\rm coh} = \exp(-xNbh_{sr}/h). \quad (56)$$

Here, $N = \nu h$ is the number of trees per unit area. According to this equation in the high-frequency approximation, the coherence factor depends on the propagation range (x), the number of trees per unit area (N), the tree radius (b), the maximum separation between the direct and ground-reflected waves (h_{sr}), and the tree's height (h). The coherence factors

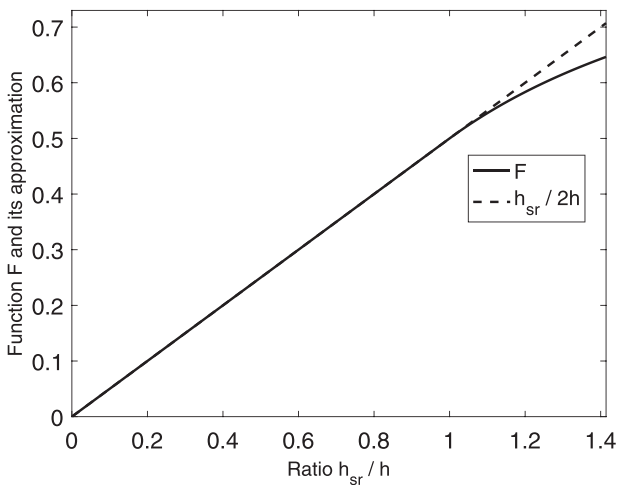

FIG. 5. Function $F(h_{sr}/h)$ and its approximation $h_{sr}/(2h)$ appearing in the coherence factor.

$C_{\rm coh}$ given by Eqs. (55) and (56) differ from that in Ref. 17 obtained by an engineering approach.

C. Numerical results

Consider the SPL relative to that in free space,

$$\mathrm{SPL} = 10\log(\langle pp^*\rangle R_1^2), \quad (57)$$

where $\langle pp^*\rangle$ is given by Eq. (48). Formulations from Sec. V B enable calculation of the SPL of the sum of the direct and ground-reflected waves in a forest. In Fig. 6, the SPL is plotted versus sound frequency f for the propagation range $x = 75$ m, and the source and receiver heights $h_s = 1$ m and $h_r = 1.5$ m. The tree height is $h = 20$ m, the number of trees per unit area is $N = 0.1\ \mathrm{m}^{-2}$, and the tree's radius is $b = 0.15$ m. With these parameters, $h_{sr}/h = 0.06$ and the function F in the exponential in Eq. (54) equals 0.094.

The normalized specific impedance of the ground is calculated with the relaxation model,[14,32]

$$Z = \frac{q}{\Omega}\left[\left(1 + \frac{\gamma - 1}{\sqrt{1 - i\omega\tau_e}}\right)\left(1 - \frac{1}{\sqrt{1 - i\omega\tau_v}}\right)\right]^{-1/2}. \quad (58)$$

Here, Ω is porosity of the ground, $q = \Omega^{-0.25}$ is tortuosity, $\tau_v = 2\varrho q^2/(\Omega\phi)$ is the vorticity relaxation time, where ϕ is the static flow resistivity, and $\tau_e = 0.709\tau v$ is the entropy relaxation time. The relationships between some of these parameters follows from Ref. 33. The static flow resistivity and porosity are chosen for the fermentation/humus layer in a forest:[34] $\phi = 52$ kPa s m^{-2} and $\Omega = 0.763$. Furthermore, in Eq. (58), $\omega = 2\pi f$ is the angular frequency, $\varrho = 1.2\ \mathrm{kg/m^3}$ is the air density, and $\gamma = 1.4$ is the ratio of the specific heats in air.

The relative SPL is plotted in Fig. 6 for the three cases: sound propagation above an impedance ground in a free

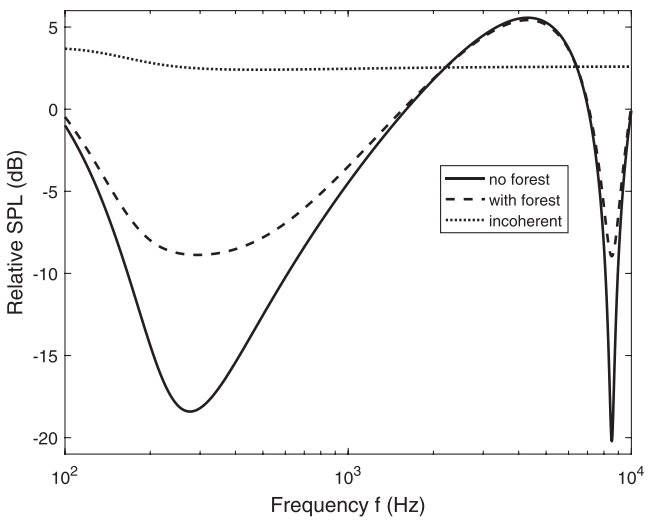

FIG. 6. Relative SPL of the sum of the direct and ground-reflected waves versus the sound frequency f. The three lines correspond to sound propagation above an impedance ground in a free atmosphere, a forest, and when the direct and ground-reflected waves are incoherent. The propagation range is $x = 75$ m, the source and receiver heights are $h_s = 1$ m and $h_r = 1.5$ m, respectively, the tree height and radius are $h = 20$ m and $b = 0.15$ m, respectively, and the number of trees per unit area is $N = 0.1\ \mathrm{m}^{-2}$.

atmosphere ($C_{\text{coh}} = 1$), for the case when the direct and ground-reflected waves are incoherent ($C_{\text{coh}} = 0$), and in a forest with parameters specified above. In the first case, the interference between the direct and ground-reflected waves results in maxima and minima of the SPL as a function of the sound frequency f. In the second case, these maxima and minima are completely suppressed and the SPL only slightly depends on the frequency. Finally, for sound propagation in a forest, the interference minima are reduced due to the coherence loss between the direct and ground-reflected waves, resulting in an apparent increase in the SPL (for this case $C_{\text{coh}} = 0.935$). Thus, the SPL of the sum of the direct and ground-reflected waves significantly depends on the coherence factor C_{coh}.

D. Comparison with experimental data

In this subsection, the theoretical results are compared with experimental data on sound propagation in different forests reported in Ref. 17.

In Figs. 7–9, black crosses represent the SPL relative to that in free space in one-third octave bands measured in a poplar forest for three propagation ranges $x = 40$ m, 60 m, and 80 m (Fig. 5 in Ref. 17). The forest had been planted, with parallel, symmetrical rows of trees. The number of trees per unit area was $N = 0.042\,\text{m}^{-2}$, the averaged tree radius was $b = 0.135$ m, and the averaged tree height was $h = 9$ m. Green crosses correspond to the SPL calculated with the Nord2000 model.[17] The predictions use the Delany-Bazley impedance model of the ground,[35] which is characterized by one parameter, the effective flow resistivity Φ. The ground impedance was not measured during the experiment, but rather Φ was used as an adjustable parameter for the best fit between theoretical and experimental data. As a result, the values of Φ were varied with range; for Figs. 7, 8, and 9, the effective flow resistivity was 90 kPa s m^{-2}, 100 kPa s m^{-2}, and 90 kPa s m^{-2}, respectively. Also, although the single-parameter nature of the Delany-Bazley model is convenient,

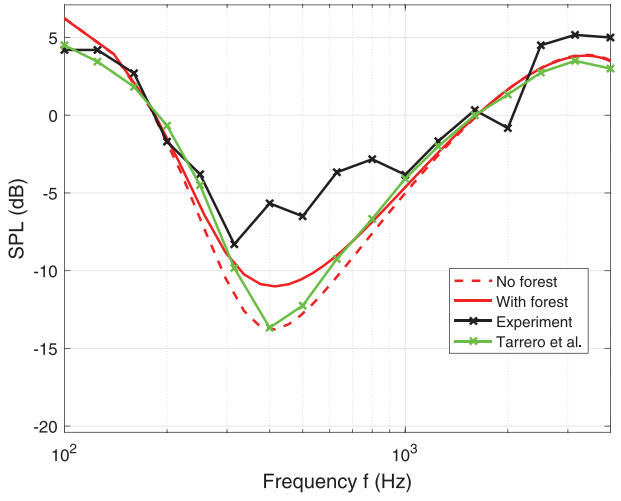

FIG. 7. Relative SPL versus the sound frequency in a poplar forest for propagation range $x = 40$ m. Black crosses are experimental data (Ref. 17), green crosses are predictions of the Nord2000 model, and the dashed and solid red lines are predictions of the current paper.

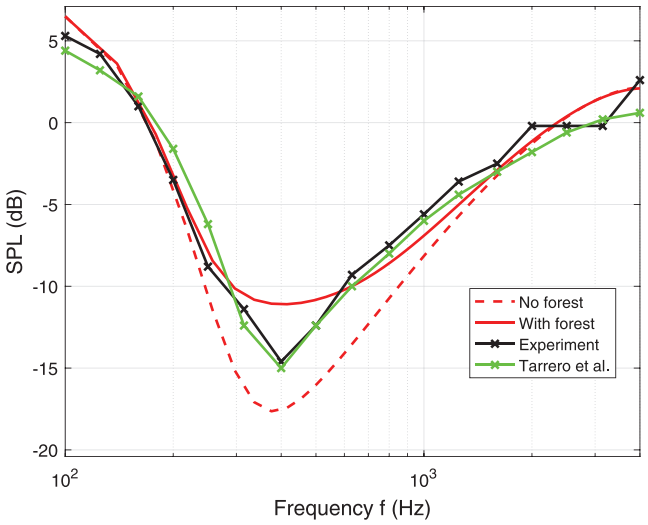

FIG. 8. Same as in Fig. 7, but for the propagation range $x = 60$ m.

it should be noted that the model is not physically admissible.[36]

In Figs. 7–9, the red lines represent the SPL calculated with Eq. (48). The dashed lines correspond to the case when scattering in the forest is ignored ($C_{\text{coh}} = 1$), while the solid lines correspond to the case when C_{coh} is calculated with Eq. (54), where N, b, and h are the parameters of the poplar forest indicated above. The ground-impedance model is an extension[37] of the relaxation model,

$$Z_{\text{gr}} = \coth(-ik_{\text{gr}}d_{\text{gr}})Z. \tag{59}$$

Here, Z is given by Eq. (58), d_{gr} is the thickness of a hard-backed porous layer, and k_{gr} is the sound wavenumber in the layer,

$$k_{\text{gr}} = \frac{q\omega}{c_0}\left(1 + \frac{\gamma - 1}{\sqrt{1 - i\omega\tau_e}}\right)^{1/2}\left(1 - \frac{1}{\sqrt{1 - i\omega\tau_v}}\right)^{-1/2}. \tag{60}$$

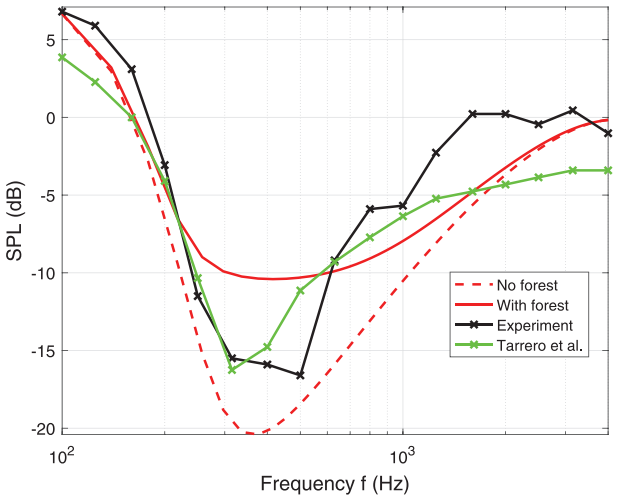

FIG. 9. Same as in Fig. 7, but for the propagation range $x = 80$ m.

The ground parameters $\phi = 110\,\text{kPa s m}^{-2}$, $\Omega = 0.7$, and $d_{\text{gr}} = 0.05\,\text{m}$ represent the best fit between the theoretical predictions and experimental data.

For $x = 40\,\text{m}$ (Fig. 7), the theory developed predicts correctly the SPL at low and high frequencies, as well as the location of the interference minimum, but overpredicts the depth of the minimum compared with the data. Note that at the interference minimum, the experimental data exhibit some fluctuations indicating that they might have been affected by one of the factors described in the next paragraph. In Fig. 7, the root mean square error (RMSE) between theoretical predictions and experimental data is 2.59 dB. The Nord2000 model predicts a deeper interference minimum with the RMSE 2.63 dB. At $x = 60\,\text{m}$ (Fig. 8), the theory developed agrees better with experimental data; the RMSE is 1.29 dB. The RMSE for the Nord2000 model is slightly smaller, 1.15 dB. For $x = 80\,\text{m}$ (Fig. 9), the theory developed underpredicts the interference dip. At this range, the RMSE is 3.36 dB, while that for the Nord2000 model is smaller, 2.60 dB.

Several factors affect the comparison between the theory and experiment. First, and probably most important, the ground impedance Z_{gr} was not measured during the experiment and might have been range dependent. Furthermore, the ground was not completely flat and homogeneous.[17] Different values of the effective flow resistivity Φ were used in Ref. 17 at different ranges, while in our predictions, the same ground parameters were used at $x = 40\,\text{m}$, 60 m, and 80 m. Second, the poplar forest was a regularly planted forest with possible sonic crystal effects. Third, the experimental data are in one-third octaves, while the theory developed is narrow band. Fourth, as mentioned in Ref. 17, refraction in the forest might have affected the experimental data at long ranges, while it is ignored both in the theory developed and the Nord2000 model. Last, but not least, modeling of trees as vertical cylinders of the same radius and height, and ignoring scattering by branches and canopy might result in some errors. A similar approach in Ref. 7 yielded good agreement between theoretical predictions and experimental data if the number of trees per unit area was reduced by 60%. To overcome this possible issue, the SCS σ_d can be measured experimentally and then used in Eq. (52) for the coherence factor C_{coh}.

Reference 17 also considers sound propagation in a pine forest and an oak forest. Though not presented here for brevity, the theory developed predicts that in the pine forest, the effect of trees on the SPL is small. This conclusion agrees with the Nord2000 model.[17] In the oak forest, the theory developed overestimates the scattering by trees as is the case for the 80 m range in the poplar forest. The probable reason is that the oak forest (Fig. 8 in Ref. 17) does not resemble vertical cylinders; a SCS σ_d different from that given by Eq. (54) should be used in this case.

VI. CONCLUSIONS

In this paper, it has been demonstrated that the equations for the statistical moments of the sound field propagating in a forest and turbulent atmosphere have the same form if, in these equations, the scattering properties of the two media are expressed in terms of the DSCS and TCS. This analogy enables the advancement of forest acoustics using results known for sound propagation in a turbulent atmosphere and vice versa; it can also be used for studies of wave propagation in many other discrete and continuous random media. Using this analogy, the following new results were obtained in the paper.

The correlation function of the sound field in a turbulent atmosphere was expressed in terms of the radiance J; see Eq. (13). The radiance satisfies the RTE, Eq. (14), where the DSCS is given by Eq. (5). This is a new result for sound propagation through a statistically inhomogeneous and anisotropic turbulence, which would be difficult to obtain with other approaches.

The second-moment PE, Eq. (47), for the correlation function of the sound field and mean intensity in a forest was obtained. This equation and the corresponding boundary conditions enable to account for temperature and wind velocity stratification in a forest and sound interaction with the impedance ground. Effective numerical techniques for solutions of the second-moment PE have been developed for sound propagation in a turbulent atmosphere and can be readily applied to forest acoustics.

For the first time, the interference of the direct and ground-reflected waves in a forest was formulated analytically. This interference was then studied numerically by modeling trunks as finite vertical solid cylinders. It was shown that sound scattering by trunks reduces the interference minima in the SPL as a function of frequency, thus, resulting in apparent increase in the SPL. Theoretical predictions were compared with experimental data presented in Ref. 17.

Other results known for sound propagation in a turbulent atmosphere can be generalized to forest acoustics. These include the variances and correlation functions of the phase and amplitude fluctuations, the spatial coherence, the frequency coherence, and pulse propagation.

The theories developed in this and companion papers[2,10,11] enable predictions of sound propagation in a forest provided that the DSCS and TCS are known. These papers consider several approaches for determining these cross sections such as modeling the trunk layer with finite vertical cylinders, branches with slanted finite cylinders, and the canopy layer with diffuse scatterers. It remains to be seen for what types of forests these approaches provide realistic DSCS and TCS. These cross sections can also be measured experimentally by comparing experimental data to theoretical predictions and retrieving DSCS and TCS. For such measurements, it seems preferable to use short pulses to separate sound scattering in a forest from ground reflection.

ACKNOWLEDGMENTS

This research was sponsored by the U.S. Army Engineer Research and Development Center, Geospatial Research and Engineering business area. Permission to publish was granted by Director, Cold Regions Research and Engineering Laboratory.

[1]K. Attenborough, K. M. Li, and K. Horoshenkov, *Predicting Outdoor Sound* (Taylor and Francis, London, 2006), pp. 1–441.
[2]V. E. Ostashev, D. K. Wilson, and M. B. Muhlestein, "Formulation of sound propagation in a forest as a radiative transfer theory," J. Acoust. Soc. Am. **142**(6), 3767–3780 (2017).

[3]D. Heimann, "Numerical simulations of wind and sound propagation through an idealised stand of trees," Acta Acust. **89**, 779–788 (2003).
[4]T. Van Renterghem, D. Botteldooren, and K. Verheyen, "Road traffic noise shielding by vegetation belts of limited depth," J. Sound Vib. **331**(10), 2404–2425 (2012).
[5]P. Chobeau, G. Guillaume, J. Picaut, D. Ecotière, and G. Dutilleux, "A transmission line matrix model for sound propagation in arrays of cylinders normal to an impedance plane," J. Sound Vib. **389** 454–467 (2017).
[6]S. Taherzadeh, I. Bashir, and K. Attenborough, "Aperiodicity effects on sound transmission through arrays of identical cylinders perpendicular to the ground," J. Acoust. Soc. Am. **132**(4), EL323–EL328 (2012).
[7]M. A. Price, K. Attenborough, and N. W. Heap, "Sound attenuation through trees: Measurements and models," J. Acoust. Soc. Am. **84**, 1836–1844 (1988).
[8]J. Defrance, N. Barrière, and E. Premat, "A diffusion model for sound propagation through forest," in *Proc. Forum Acusticum*, Sevilla, Spain (2002).
[9]M. E. Swearingen and M. J. White, "Influence of scattering, atmospheric refraction, and ground effect on sound propagation through a pine forest," J. Acoust. Soc. Am. **122**, 113–119 (2007).
[10]V. E. Ostashev, D. K. Wilson, and M. B. Muhlestein, "Effective wavenumbers for sound scattering by trunks, branches, and canopy in a forest," J. Acoust. Soc. Am. **142**(2), EL177–EL183 (2017).
[11]M. B. Muhlestein, V. E. Ostashev, and D. K. Wilson, "Acoustic pulse propagation in forests," J. Acoust. Soc. Am. **143**(2), 968–979 (2018).
[12]A. Ishimaru, *Wave Propagation and Scattering in Random Media* (IEEE, New York, 1997), pp. 1–572.
[13]L. A. Apresyan and Yu. A. Kravtsov, *Radiation Transfer* (Gordon and Breach, Amsterdam, 1996), pp. 1–456.
[14]V. E. Ostashev and D. K. Wilson, *Acoustics in Moving Inhomogeneous Media*, Second ed. (CRC Press, Boca Raton, FL, 2015), pp. 1–521.
[15]R. Bullen and F. Fricke, "Sound propagation through vegetation," J. Sound Vib. **80**, 11–23 (1982).
[16]W. H. T. Huisman and K. Attenborough, "Reverberation and attenuation in a pine forest," J. Acoust. Soc. Am. **90**, 2664–2677 (1991).
[17]A. I. Tarrero, M. A. Martin, J. Gonzalez, M. Machimbarrena, and F. Jacobsen, "Sound propagation in forests: A comparison of experimental results and values predicted by the Nord 2000 model," Appl. Acoust. **69**, 662–671 (2008).
[18]G. A. Daigle, "Effects of atmospheric turbulence on the interference of sound waves above a finite impedance boundary," J. Acoust. Soc. Am. **65**, 45–49 (1979).
[19]S. F. Clifford and R. J. Lataitis, "Turbulence effects on acoustic wave propagation over a smooth surface," J. Acoust. Soc. Am. **73**(5), 1545–1550 (1983).
[20]E. Salomons, V. E. Ostashev, S. Clifford, and R. Lataitis, "Sound propagation in a turbulent atmosphere near the ground: An approach based on the spectral representation of refractive index fluctuations," J. Acoust. Soc. Am. **109**, 1881–1893 (2001).
[21]V. E. Ostashev, E. Salomons, S. Clifford, R. Lataitis, D. K. Wilson, Ph. Blanc-Benon, and D. Juvé, "Sound propagation in a turbulent atmosphere near the ground: A parabolic equation approach," J. Acoust. Soc. Am. **109**, 1894–1908 (2001).
[22]I. Bashir, S. Taherzadeh, H.-C. Shin, and K. Attenborough, "Sound propagation over soft ground with and without crops and potential for surface transport noise reduction," J. Acoust. Soc. Am. **137**, 154–164 (2015).
[23]Z. Ye, "A novel approach to sound scattering by cylinders of finite length," J. Acoust. Soc. Am. **102**, 877–884 (1997).
[24]*3D Radiative Transfer in Cloudy Atmospheres*. edited by A. Marshak and A. B. Davis (Springer, New York, 2005), pp. 1–686.
[25]S. M. Rytov, Yu. A. Kravtsov, and V. I. Tatarskii, *Principles of Statistical Radio Physics. Part 4, Wave Propagation through Random Media* (Springer, Berlin, 1989), pp. 1–188.
[26]D. K. Wilson and V. E. Ostashev, "Statistical moments of the sound field propagating in a random, refractive medium near an impedance boundary," J. Acoust. Soc. Am. **109**, 1909–1922 (2001).
[27]D. K. Wilson, V. E. Ostashev, and M. S. Lewis, "Moment-screen method for sound propagation in a refractive medium with random scattering," Waves Random Complex Media **19**(3), 369–391 (2009).
[28]S. Cheinet, "A numerical approach to sound levels in near-surface refractive shadows," J. Acoust. Soc. Am. **131**, 1946–1958 (2012).
[29]A. D. Pierce, *Acoustics: An introduction to its Physical Principles and Applications* (American Institute of Physics, Melville, NY, 1994), pp. 1–642.
[30]P. M. Morse and K. U. Ingard, *Theoretical Acoustics* (McGraw-Hill, New York, 1968), pp. 1–949.
[31]A. Ziemann, M. Barth, and M. Hehn, "Experimental investigation of the meteorologically influenced sound propagation through an inhomogeneous forest site," Meteorol. Z. **22**(2), 221–229 (2013).
[32]D. K. Wilson, "Simple relaxation models for the acoustical properties of porous media," Appl. Acoust. **50**, 171–188 (1997).
[33]V. E. Ostashev, D. K. Wilson, and S. N. Vecherin, "Effect of random impedance on the interference of the direct and ground-reflected waves," J. Acoust. Soc. Am. **130**(4), 1844–1850 (2011).
[34]M. J. M. Martens, L. A. M. van der Heijden, H. H. J. Walthaus, and W. J. J. M. van Rens, "Classification of soils based on acoustic impedance, air flow resistivity, and other physical soil parameters," J. Acoust. Soc. Am. **78**, 970–980 (1985).
[35]M. E. Delany and E. N. Bazley, "Acoustical properties of fibrous absorbent materials," Appl. Acoust. **3**(2), 105–116 (1970).
[36]D. Dragna, K. Attenborough, and P. Blanc-Benon, "On the inadvisability of using single parameter impedance models for representing the acoustical properties of ground surfaces," J. Acoust. Soc. Am. **138**, 2399–2413 (2015).
[37]K. Attenborough, I. Bashir, and S. Taherzadeh, "Outdoor ground impedance models," J. Acoust. Soc. Am. **129**(5), 2806–2819 (2011).